ELSEVIER

Biochemical Engineering Journal 2 (1998) 145–155

Biochemical Engineering Journal

Mathematical modeling and scale-up of size-exclusion chromatography

Zhiguo Li, Yesong Gu, Tingyue Gu*

Department of Chemical Engineering, Ohio University, Athens, OH 45701-2979, USA

Received 5 March 1998; accepted 5 August 1998

Corrected.

Abstract

Size exclusion chromatography (SEC) is a widely used tool in bioseparations. Because its separation mechanism is based on the permeability of macromolecules rather than any type of binding, the feed volume to bed volume ratio is usually quite small. Thus, large columns are typically used in preparative- and large scale separations. In this work, a general rate model considering various mass transfer effects was successfully used for the scale-up predictions of preparative SEC columns. The effects of various physical parameters on the performance of SEC were investigated using computer simulation based on the model. A method was developed to scale up SEC columns based on a few simple elution runs on a small column with the same packing to be used in the larger column using a personal computer based simulation software program. Existing correlations in the literature were used to estimate some mass transfer coefficients in the general rate model. The elution peaks for a large column could be predicted a priori using the method which was tested experimentally in this work. It very accurately predicted the retention times and peak shapes of myoglobin and ovalbumin eluted from three preparative SEC glass columns packed with P60 gel (Bio-Rad Laboratories, Hercules, CA, USA). The bed dimensions were 4.4 cm(i.d.)×29.5 cm, 5.0 cm×29.5 cm, and 5.0 cm×42.0 cm, respectively. The small column used for the scale-up prediction had bed dimensions of 1.5 cm×27.3 cm.

Keywords: Size exclusion; Chromatography; Model; Scale-up

1. Introduction

Size exclusion chromatography (SEC) is also referred to as gel permeation or gel filtration chromatography [1,2]. It separates macromolecules on the basis of their relative size or hydrodynamic volumes. Since its introduction in 1964 [3], SEC has long proven to be an indispensable tool for the analysis and separation of macromolecules such as proteins and polymers. SEC is widely used as a tool for the preparative and large-scale separation and purification of macromolecules [4,5]. Many commercial bioseparation processes consist one or more steps of SEC [6]. Because SEC does not rely on any binding between solutes and the stationary phase, its feed volume is very limited compared to other forms of chromatography such as reversed-phase and ion-exchange chromatography. This is the reason why commercial scale SEC columns tend to be very large, with bed volumes reaching hundreds of liters.

Because soft gels are typically used as the packing media, column height expansion is limited due to pressure limitation. Thus, large SEC columns tend to have large diameters in order to accommodate large feed volumes. In such columns, diffusional and mass transfer effects can be significant. A number of monographs have been published [7–11] on the theories and applications of SEC. Several mathematical models that consider mass transfer effects exist in the literature [12–15]. Kim and Johnson's model introduced a 'pore volume fraction' to account for the size exclusion effect of particles. Similar to this, Gu [12] proposed the use of an accessible particle porosity (i.e., accessible macropore volume fraction for a macromolecule) to describe the effect of size exclusion in a general rate model which considers axial dispersion, interfacial film mass-transfer and intraparticle diffusion. Similar general rate models were used by Liapis and Arve [16,17] in affinity chromatography, and Yu and Wang for ion-exchange chromatography [18]. In this work, a personal computer (PC) based FORTRAN 77 software program [12] using the general rate model was used for the simulation and scale-up of SEC. In the model, accessible particle porosity and tortuosity data were correlated by matching elution data from a small SEC column using computer simulation. Other mass transfer parameters were

*Corresponding author.

1369-703X/98/$ – see front matter
PII: S1369-703X(98)00027-8

calculated using existing correlations. Based on these data, elution peaks were predicted for a larger column using the software without any posterior data from the larger column. Parameter sensitivities were investigated by studying the effects of the parameters using computer simulation. Experimental single-component and binary elution profiles for a 4.4 cm(i.d.)×29.5 cm (bed dimensions) SEC column, a 5.0 cm×29.5 cm SEC column, and a 5.0 cm×42.0 cm SEC column were accurately predicted based on elution data from a small 1.5 cm×27.3 cm (bed dimensions) column packed with the same gel.

2. Mathematical model

The general rate model for SEC considers the following three mass transfer processes in the SEC column.

1. Axial dispersion in the bulk-fluid phase,
2. interfacial film mass-transfer between the stationary and mobile phases, and
3. diffusion of solutes within the macropores of the packing particles.

2.1. Model assumptions

The following assumptions are needed to formulate the model:

1. The column is isothermal,
2. there is no interaction between different solutes,
3. diffusion and mass-transfer coefficients remain constant,
4. packing particles can be treated as spherical and uniform in size,
5. the packing density is even along the column, and
6. diffusion in the radial direction is negligible.

In this work, particles are viewed as having a nominal particle size and a nominal pore diameter. It is too complicated to use a particle size distribution and a pore size distribution to describe particles.

2.2. Model formulation

With the aforementioned assumptions, the following governing equations can be formulated from differential mass balances for a solute in the bulk-fluid phase and the particle phase, respectively.

$$-D_b\frac{\partial^2 C_b}{\partial Z^2}+v\frac{\partial C_b}{\partial Z}+\frac{\partial C_b}{\partial t}+\frac{3k(1-\varepsilon_b)(C_b-C_{p,R=R_p})}{\varepsilon_b R_p}=0 \quad (1)$$

$$\frac{\partial C_p}{\partial t}=D_p\left(\frac{\partial^2 C_p}{\partial R^2}+\frac{2}{R}\frac{\partial C_p}{\partial R}\right) \quad (2)$$

Eqs. (1) and (2) have the following initial and boundary conditions,

$$t=0,\ C_b=C_b(0,R,Z),\ C_p=C_p(0,R,Z)$$

$$Z=0,\ \frac{\partial C_b}{\partial Z}=\frac{v}{D_b}[C_b-C_f(t)];\ Z=L,\ \frac{\partial C_b}{\partial Z}=0$$

$$R=0,\ \frac{\partial C_p}{\partial R}=0;\ R=R_p,\ \frac{\partial C_p}{\partial R}=\frac{k}{\varepsilon_p^a D_b}(C_b-C_{p,R=R_p})$$

By introducing the following dimensionless terms,

$$z=Z/L,\ \tau=vt/L,\ r=R/R_p,\ c_b=C_b/C_0,\ c_p=C_p/C_0$$

and,

$$\mathrm{Pe_L}=vL/D_b,\ \mathrm{Bi}=kR_p/(\varepsilon_p^a D_p),\ \eta=\varepsilon_p^a D_p L/(R_p^2 v),$$
$$\xi=3\mathrm{Bi}\eta(1-\varepsilon_b)/\varepsilon_b$$

Eqs. (1) and (2) can be transformed into the following forms,

$$-\frac{1}{\mathrm{Pe_L}}\frac{\partial^2 c_b}{\partial z^2}+\frac{\partial c_b}{\partial \tau}+\frac{\partial c_b}{\partial z}+\xi(c_b-c_{p,r=1})=0 \quad (3)$$

$$\frac{\partial c_p}{\partial \tau}=\frac{\eta}{\varepsilon_p^a}\left(\frac{\partial^2 c_p}{\partial r^2}+\frac{2}{r}\frac{\partial c_p}{\partial r}\right) \quad (4)$$

with dimensionless initial conditions,

$$\tau=0,\ c_b=c_b(0,r,z,),\ c_p=c_p(0,r,z)$$

and dimensionless boundary conditions,

$$z=0,\frac{\partial c_b}{\partial z}=\mathrm{Pe_L}\left[c_b-\frac{C_f(\tau)}{C_0}\right]$$

where,

$$\frac{C_f(\tau)}{C_0}=\begin{cases}1 & 0\le\tau\le\tau_{imp}\\ 0 & \text{else.}\end{cases}$$

τ_{imp} is the dimensionless time duration for a rectangular sample pulse.

At

$$z=1,\ \frac{\partial c_b}{\partial z}=0$$

and at $r=0,\ \partial c_p/\partial r=0$; at $r=1,\ \partial c_p/\partial r=\mathrm{Bi}(c_b-c_{p,r=1})$

This dimensionless partial differential equation system was solved numerically [12] using FORTRAN 77 on a personal computer. Quadratic finite elements were used to discretize Eq. (3). The orthogonal collocation method was used to discretize Eq. (4). The resulting ordinary differential equation (ODE) system was solved using an ODE solver called DVODE authored by Peter N. Brown, Alan C. Hindmarsh, and George D. Byrne [19]. Depending on the stiffness of peak profiles computation time ranges from seconds to minutes on a Pentium-150 MHz PC. The model system is expressed for one solute. Since it is assumed that there is no interaction between the solutes, the elution profiles for different solutes can be calculated independently. The FORTRAN 77 can simulate multi-component elutions in a single execution by calculating the elution profiles simultaneously.

2.3. Model input parameters

The input data for the FORTRAN 77 code include the number of components, the number of elements (Ne), the number of interior collocation points (Nc), τ_{imp} (injection volume in terms of dimensionless feed time), particle porosity (ε_p), the bed void volume fraction (ε_b), the Peclet number (Pe_L), the η number, the Biot number (Bi), the maximum concentration (C_0, usually the feed concentration for simple column operations) and the size exclusion factor (F^{ex}).

2.3.1. Numerical parameters (Ne and Nc)

If the number of elements (Ne) is too small, the simulated elution peaks will have oscillation. If it is too large, excessive computation time is used. The general rule is that the stiffer the concentration profiles the higher the Ne value. A small Ne value can be tried out first. If the solution shows oscillation, a larger value for Ne can be used. For stiff cases, Ne = 20–30 is often enough.

The value of Nc does not affect the stability of the numerical solution. Usually, two interior collocation points (Nc = 2) are needed, especially when D_p values are small. Sometimes one interior collocation point is sufficient for practical applications.

2.3.2. Bed void volume fraction (ε_b)

The value of ε_b depends on the size of the packing particles, as well as the packing procedure. In this work, ε_b was treated as a constant for different columns with the same packing material. ε_b can be obtained experimentally according to the following relationship,

$$t_d = L/v = \frac{\pi d^2 L \varepsilon_b}{4Q} \tag{5}$$

in which t_d is the retention time of very large molecules such as blue dextran which is completed excluded from the macropores. t_d is also known as the dead-volume time.

2.3.3. Particle porosity (ε_p)

The value of ε_p can be calculated from the retention time or the elution volume of a small molecule whose size is smaller than the lower exclusion limit of the porous particles. The relationship between the retention time of a small solute t_0 and ε_p is shown in Eq. (6).

$$t_0 = t_d\left[1 + \frac{(1-\varepsilon_b)\varepsilon_p}{\varepsilon_b}\right] \tag{6}$$

2.3.4. Accessible particle porosity for a solute (ε_p^a)

The accessible particle porosity represents the accessible macropore volume fraction (vs. the total particle volume) for a particular solute. ε_p^a value for a typical macromolecule such as a protein is less than ε_p. This means that the protein molecule can penetrate some larger pores while it is excluded from smaller pores. If a macromolecule has $\varepsilon_p^a = 0$, it means that this molecule is completely excluded from the macropores. Blue dextran is an example. The ε_p^a value of a solute differing from that of another solute is a key factor responsible for the separation of molecules in an SEC column. The value of ε_p^a for a solute can be obtained from its retention time (t_R) using Eq. (7).

$$t_R = t_d\left[1 + \frac{(1-\varepsilon_b)\varepsilon_p^a}{\varepsilon_b}\right] \tag{7}$$

2.3.5. Peclet number (Pe_L)

$$Pe_L = \frac{L}{2R_p\varepsilon_b}(0.2 + 0.011Re^{0.48}),\ 10^{-3} \le Re \le 10^3 \tag{8}$$

According to the definition of Peclet number ($Pe_L = vL/D_b$), its value can be calculated from the axial dispersion coefficient (D_b). However, the value of D_b is not easy to measure experimentally. In this work, Pe_L was calculated according to the Chung and Wen [20] correlation for a fixed bed. where, $Re = (2R_p)v\rho/\mu$. When Re is small, the contribution to Pe_L from the second term in the brackets is negligible. For instance, the elimination of the second term produces a 0.8% error when Re equals 0.02. In all the experiments of this work, Re is less than 0.02. Therefore, Eq. (8) can be written as

$$Pe_L = \frac{vL}{D_b} = \frac{0.1L}{R_p\varepsilon_b},\ Re \le 0.02 \tag{9}$$

2.3.6. η number

In order to calculate the value of η number [$\eta = \varepsilon_p^a D_p L/(R_p^2 v)$], the value of effective diffusivity (D_p) is needed. D_p affects peak widths in chromatograms. D_p can be obtained from the molecular diffusivity (D_m) [21,22]. In this work, the following correlation [21] is used.

$$D_p = \frac{D_m}{\tau_{tor}}(1 - 2.104\lambda + 2.09\lambda^3 - 0.95\lambda^5) \tag{10}$$

In Eq. (10), in order to calculate the value of D_p, the value of the pore tortuosity (τ_{tor}), the molecular diffusivity (D_m) and the ratio of the solute molecular diameter to the pore diameter λ are needed. The value of τ_{tor} for gas diffusion into porous materials is easy to obtain [23]. However, no rigorous expression of τ_{tor} is available for liquids; it has to be obtained experimentally.

The molecular diffusivity (D_m) of large spherical molecules is given by the Stokes–Einstein equation [24] as

$$D_m = \frac{\kappa T}{6\pi\mu R_m} \tag{11}$$

where κ is the Boltzmann constant and T is the absolute temperature.

The radius of a solute molecule can be obtained from its specific volume (v_s) and its molecular weight based on the assumption that the protein is spherical. It can be written

as

$$R_m = \left[\frac{3(MW)v_s}{4\pi N}\right]^{1/3} \quad (12)$$

According to Marshall [25] the v_s values of proteins are in a narrow range (0.728~0.751). If v_s is assigned an average value of 0.7384, then,

$$R_m(\text{Å}) = 0.66(MW)^{1/3} \quad (13)$$

Usually proteins in solutions are hydrated and this results in an increase of their sizes [26]. If the hydrodynamic radius is assumed proportional to $(MW)^{1/3}$, the following semi-empirical relationship [27] can be obtained from Eq. (11),

$$D_m(m^2/s) = C/(MW)^{1/3} \quad (14)$$

Using Eq. (14) to fit experimental data for some organic substances including proteins such as bovine serum albumin (BSA), hemoglobin and myoglobin, Polson [27] correlated their C values. He found that the C values averaged 2.74×10^{-9} s m^{-2} with a quite small deviation for organic substances with MW greater than 1000. Thus he proposed the following relationship,

$$D_m(m^2\,s^{-1}) = 2.74\times10^{-9}(MW)^{-1/3} \quad (15)$$

Eq. (15) was adopted to calculate D_m in this work because of its simplicity and good accuracy for proteins similar to those used in this work.

The pore diameter of the gel (d_{pore}) may be provided by manufacturers, but for most soft porous materials, it is usually unavailable. In this case, an approximation for the pore diameter of the gel can be obtained from the upper exclusion limit of the gel. For polymers, the value of λ is a function of the molecular weight of a solute [11]. Here, a simple method was used to calculate the value of λ for a solute assuming spherical molecules, cylindrical pores, and equal partial specific volume,

$$\lambda = d_m/d_{pore} = \lambda_0\left[\frac{\text{MW of solute molecule}}{\text{MW of upper exclusion limit}}\right]^{1/3} \quad (16)$$

where $\lambda_0 = 0.35$ according to Stegeman et al. [28]. This equation was derived using Eq. (13) by assuming that when the solute diameter reaches 35% of the pore diameter, it is unable to penetrate the pore [28]. In this work, the MW of upper exclusion limit for the Bio-Rad P60 gel (Bio-Rad Laboratories, Hercules, CA, USA) was set to 67,000 which is the MW of BSA. This is because experiments showed that BSA has very limited access to the pores of P60 gel used in this work. The ε_p^a value for BSA is only 0.03 which means only a small fraction of the pores are large enough for BSA to penetrate. The P60 gel has a nominal size exclusion MW range of 3000 to 60,000 according to its vendor. If 60,000 is chosen instead of 67,000, there will be no significant error in the simulated elution profiles.

2.3.7. Biot number (Bi) for mass transfer

The value of Bi[$\text{Bi} = kR_p/(\varepsilon_p^a D_p)$] can be obtained from the effective diffusivity (D_p) and the film mass-transfer coefficient (k). The value of D_p is calculated from Eq. (10). Under normal experimental conditions of an SEC column, the Reynolds number is usually very small. Several correlations can be employed to estimate the value of the film mass-transfer coefficient (k) in terms of the Sherwood number (Sh) for small Re. The following equation [29] seems to be most convenient since viscosity cancels out in Re·Sc,

$$\text{Sh} = \frac{1.09}{\varepsilon_b}(\text{Re}\cdot\text{Sc})^{0.33} = 1.37(\varepsilon_b v R_p/D_m)^{0.33}/\varepsilon_b,\ 0.0015 \le \text{Re} \le 55 \quad (17)$$

where
$\text{Sh} = (2R_p)k/D_m$, $\text{Sc} = \mu/(D_m\rho)$ and $\text{Re} = (2R_p)\rho v\varepsilon_b/\mu$.
After Sh value is obtained, k value can be calculated from $k = \text{Sh}\cdot D_m/(2R_p)$.

2.3.8. Size-exclusion factor (F^{ex})

The size-exclusion factor ($F^{ex} = \varepsilon_p^a/\varepsilon_p$) introduced by Gu [12] actually has the same value as of the distribution coefficient (K_{SEC}). The separation capacity of an SEC column can be characterized by K_{SEC} which is defined [30] using solute elution volume (V_e),

$$K_{SEC} = \frac{V_e - V_0}{V_t - V_0} \quad (18)$$

K_{SEC} can also be written as,

$$K_{SEC} = \frac{t_R - t_d}{t_0 - t_d} \quad (19)$$

Inserting Eqs. (6) and (7) into Eq. (19) yields,

$$K_{SEC} = \frac{\varepsilon_p^a}{\varepsilon_p} \quad (20)$$

Thus, F^{ex} has the same value as K_{SEC}. F^{ex} can be readily calculated using ε_p^a and ε_p values.

3. Effects of mass transfer parameters on SEC performance

It is beneficial to find out the sensitivities of parameters in the model system. The results can indicate which parameters are relatively important and should be more accurately estimated for the model system, and which parameters do not require rigid estimation.

3.1. Effect of the Peclet number (Pe_L)

The value of Pe_L represents the extent of the axial dispersion. As Pe_L approaches infinity, the axial dispersion becomes negligible, indicating a plug flow. The influence of Pe_L on the simulated chromatogram is shown in Fig. 1.

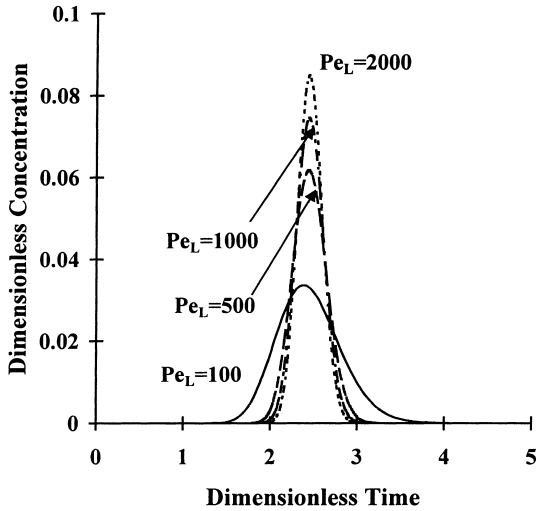

Fig. 1. The effect of Pe_L number.

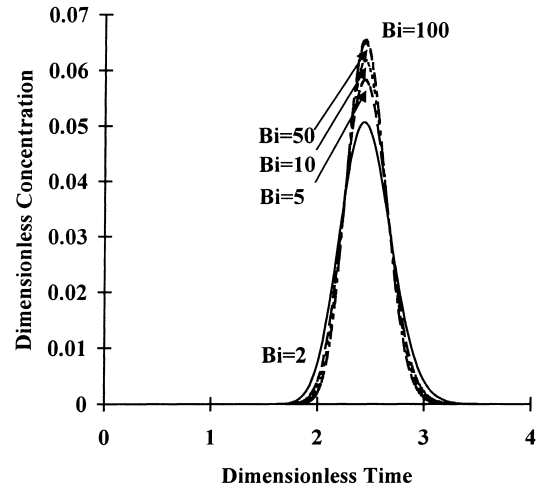

Fig. 2. The effect of Biot number.

Parameters used in computer simulation to obtain Fig. 1 are listed in Table 1. In addition, $\varepsilon_p = 0.6$, $\varepsilon_b = 0.26$, F^{ex}=0.8 and τ_{imp}=0.03 were used. From Fig. 1, it can be seen that, when Pe_L becomes larger, the simulated peak becomes sharper. When Pe_L exceeds 1000, its influence on peak width becomes relatively insignificant. This case is always true in this work. Because the value of Re is quite small, the Pe_L value calculated from Eq. (9) is above 1000.

3.2. Effect of the Biot number (Bi)

The value of Bi reflects the characteristic ratio of the external film mass-transfer rate to the intraparticle diffusion rate. The effect of Bi on elution peak is shown in Fig. 2. It appears that Bi plays almost no part in the overall peak broadening effect when its value is greater than 50. This large Bi value indicates that the mass transfer process is limited by intraparticle diffusion. Interfacial mass transfer resistance is negligible in such cases. In all the experiments in this work, Bi was greater than 50, thus its influence on peak broadening was relatively insignificant.

Table 1
Parameter values used for the study of effects of Pe_L, Bi and η

Figures	Simultation parameters			Numerical parameters	
	Pe_L	Bi	η	Nc	Ne
Fig. 1	100	10	10	2	22
	500				
	1000				
	2000				
Fig. 2	500	2	10	2	20
		5			
		10			
		50			
		100			
Fig. 3	500	10	0.5	2	20
			5		
			10		
			50		
			100		

3.3. Effect of the η number

The η number $[\eta = \varepsilon_p^a D_p L/(R_p^2 v)]$ plays an important role in the peak skewness and peak width. Fig. 3 shows that the peak shape is sensitively affected by the value of η. The larger the η value, the sharper the peak. When η decreases, the simulated peak first broadens then appears skewed.

3.4. The effect of particle radius (R_p)

The particle radius of an SEC gel is a very important factor that affects peak broadening. From Fig. 4, it is seen

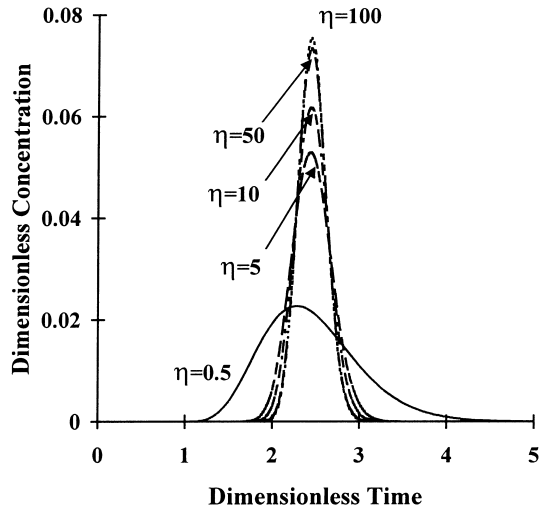

Fig. 3. The effect of η number.

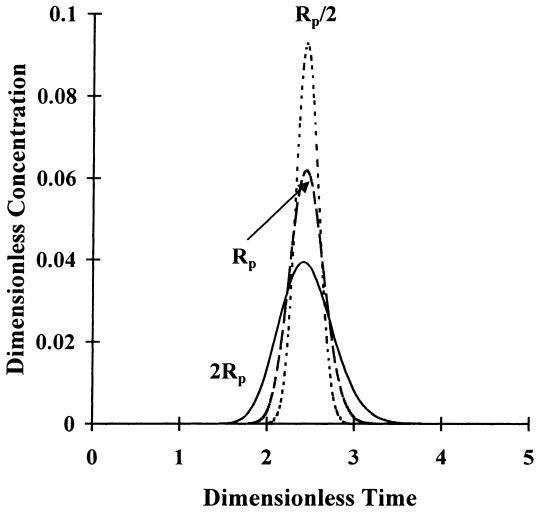

Fig. 4. The effect of particle radius (R_p).

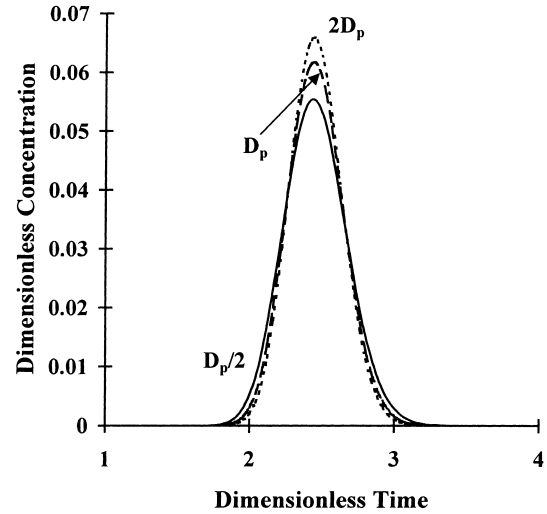

Fig. 5. The effect of effective diffusion coefficient (D_p).

that a smaller particle radius makes the simulated peak stiffer and hence provides a better resolution. In Fig. 4, the $R_p/2$ peak means that it is calculated using dimensionless parameters Pe_L, Bi, and η values that reflect a reduction of 50% in particle radius (see Table 2). The drawback of a small particle size is that column pressure goes up. This may result in excessive bed compression.

3.5. Effect of the effective diffusion coefficient (D_p)

Fig. 5 shows the influence of D_p on peak broadening. It is seen that a larger D_p value gives a sharper peak. Eq. (10) shows that D_p increases with the decrease of λ when $0 < \lambda < 1$. According to Eq. (16), a lower λ value implies a larger pore diameter of the packing particle. So a larger pore size results in sharper peaks. However, selection of pore size also relies on how effective the pore size can discriminate against different solute molecules to be separated.

3.6. Effect of the pore tortuosity (τ_{tor})

According to Eq. (10), the pore tortuosity influence the performance of an SEC column through D_p. D_p increases with the decrease of τ_{tor}. Therefore, a larger pore tortuosity gives a broader peak. The effect of τ_{tor} is shown in Fig. 6. τ_{tor} value range is quite broad. It is not easily estimated. Thus in this work, it is correlated by matching experimental elution profile from a small column with the profile calculated using computer simulation with the rate model. The same τ_{tor} value is used for larger beds with the same packing material. By adjusting τ_{tor}, some errors resulting from the estimation of diffusional mass transfer parameters may be alleviated to a certain degree.

4. Experimental

The validity of a model can be judged by its ability to predict actual experimental results. In this work, the Bio-Rad P60 gel was used as the packing material. Three glass

Table 2
Parameter values used for study of the effects of R_p, D_p and τ_{tor}

Figures	Physical parameters	Simulation parameters			Numerical parameters	
		Pe_L	Bi	η	Nc	Ne
Fig. 4	$R_p/2$	100	7.94	40	2	24
	R_p	500	10	10		
	$2R_p$	250	12.6	2.5		
Fig. 5	$D_p/2$	500	20	5	2	20
	D_p	500	10	10		
	$2D_p$	500	5	20		
Fig. 6	$6\tau_{tor}$	500	60	2	2	20
	$3\tau_{tor}$	500	30	4		
	$2\tau_{tor}$	500	20	6		
	τ_{tor}	500	10	12		

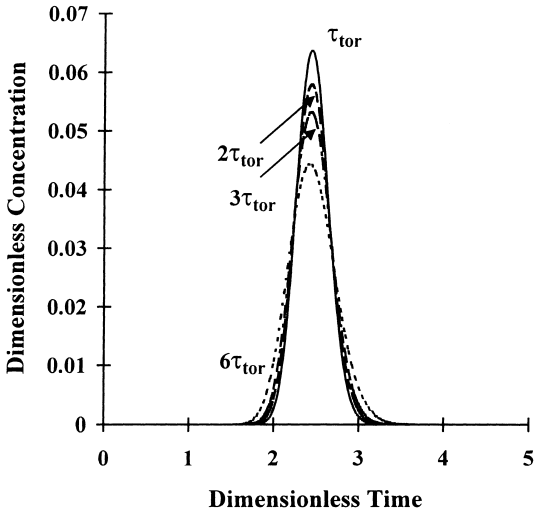

Fig. 6. The effect of particle tortuosity (τ_{tor}).

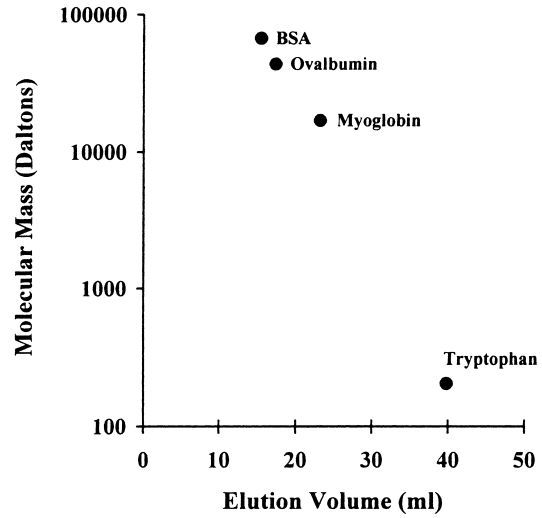

Fig. 7. The calibration curve for a small SEC column (1.5 cm×30 cm bed dimensions).

columns were employed: a 1.5 cm×80 cm Bio-Rad column, a 5 cm×70 cm Bio-Rad column and a 4.4 cm×50 cm Amicon column (Amicon, Beverly, MA, USA). BSA, myoglobin and ovalbumin (Sigma, St. Louis, MO, USA) were used. All experiments were carried out at ambient temperature using a Cole Parmer Marsterflex pump (Cole Parmer, Chicago, IL, USA). Fractions of the column effluent were collected using a Bio-Rad 2110 fraction collector. Protein concentration analysis was done using a Beckman DU640 spectrophotometer (Beckman Instrument, Fullerton, CA, USA).

The elution volume is more reliably measured than the retention time, because the elution volume is more stable for a solute in different runs. Therefore, in order to calculate ε_b, ε_p and ε_p^a Eqs. (5)–(7) are rewritten as,

$$V_{e,d} = \pi d^2 L \varepsilon_b / 4 \tag{21}$$

$$V_{e,0} = V_{e,d}\left[1 + \frac{(1-\varepsilon_b)\varepsilon_p}{\varepsilon_b}\right] \tag{22}$$

$$V_{e,R} = V_{e,d}\left[1 + \frac{(1-\varepsilon_b)\varepsilon_p^a}{\varepsilon_b}\right] \tag{23}$$

In this work, ε_b, ε_p, ε_p^a and τ_{tor} were obtained using a small column. Since these parameters are properties of the gel particles rather than a bed, the same values obtained from a small column can be used for a large bed as long as the same gel is used and the bed compression is not very different between the two beds. Note that each solute has its own ε_p^a value.

5. Results and discussions

5.1. Calibration curve

Fig. 7 shows the experimental calibration curve for protein samples on a 1.5 cm×30 cm (bed dimensions) glass column packed with the Bio-Rad P60 gel. The sample molecules were BSA, ovalbumin, myoglobin and L-tryptophan. Tryptophan (MW=204) was small enough for P60 gel such that it was not excluded by any pores. This curve was used to calculate the values of ε_p and ε_p^a. Blue Dextran was used to measure the void volume fraction of the column (ε_b). The values of ε_b, ε_p, and ε_p^a for a protein (such as ovalbumin and myoglobin) were calculated according to Eqs. (21)–(23), respectively using experimental elution volumes of blue dextran, tryptophan, and the solute protein. The elution volumes were easily obtained by measuring the retention volumes on experimental chromatograms. The results are listed in Table 3.

5.2. Determination of the pore tortuosity (τ_{tor})

τ_{tor} value for the P60 gel was obtained by matching a model calculated peak profile with its corresponding experimental peak profile on the small column (1.5 cm×30 cm bed dimensions). An assumed τ_{tor} value was first used in the computer program to calculate the peak profile. If the simulated peak had a wider band width compared to that of the experimental peak. A smaller τ_{tor} was used to run the

Table 3
Values of physical parameters used in scale-up

Proteins	MW	ε_p^a	F^{ex}	$D_m\times10^{11}$ ($m^2\,s^{-1}$)	$D_p\times10^{11}$ ($m^2\,s^{-1}$)	ε_b	ε_p	τ_{tor}	$R_p\times10^6$ (m)
Myoglobin	16890	0.23	0.35	10.7	2.98	0.27	0.66	2.0	67.5
Ovalbumin	43500	0.08	0.12	7.8	1.65				

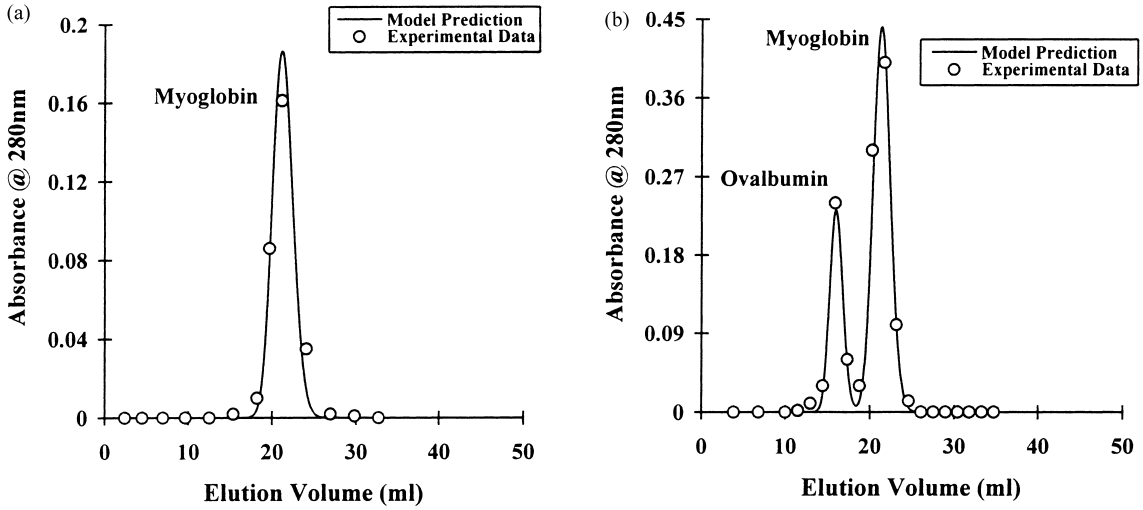

Fig. 8. Comparison between experimental results and model predictions for a small column(1.5 cm×27.3 cm bed dimensions). (a) single component elution; (b) binary elution.

computer program again until the two peaks match. For Bio-Rad P60 gel used in this work, the value of τ_{tor} was found to be 2.0 in Fig. 8(a).

5.3. Scale-up procedure

If a large column is to be built or purchased, the column's performance can be evaluated using the computer software. Three elution experiments are carried out using a small column with the same packing. Elution experiments are carried out using blue dextran, a small molecule (such as an amino acide) and some of the proteins to be separated. With the experimental elution volumes for these molecules, ε_b, ε_p, and ε_p^a (for individual proteins) values can be easily calculated using Eqs. (21)–(23). A calibration curve similar to Fig. 7 can be produced. Not all proteins need to be experimentally tested for their ε_b^a values, since their values may be interpolated using the calibration curve.

In the general rate model, with an assumed τ_{tor} value, D_p can be calculated using Eq. (10) and because it is a particle-specific parameter, it can be used for both small and large columns for the same protein. Thus, η is readily calculated using its definition, $[\eta = \varepsilon_p^a D_p L/(R_p^2 v)]$. R_p value is usually from the vendor of the packing material. Pe_L is conveniently calculated using Eq. (9). In order to calculate the Biot number for mass transfer, $Bi = kR_p/(\varepsilon_p^a D_p)$, the film mass transfer coefficient k for a protein is needed. It is calculated from the Sh value obtained from Eq. (17).

The ε_b, ε_p, and ε_p^a and τ_{tor} values obtained for the small column can be then used to calculate the elution profiles for a larger column. Different bed size and operational conditions can be simulated. The predicted elution profiles form the basis of choosing or specifying the larger column.

5.4. Experimental scale-up example

To validate the scale-up procedure, a small column(1.5 cm×27.3 cm bed dimensions) packed with P60 gel was used. Comparisons between the model calculated and the experimental results on the small column are shown in Fig. 8(a) and (b). Fig. 8(a) shows the results for a single-component elution. Jtor value was adjusted to allow a good fit between model calculated and experimental data. This τ_{tor} value was then used for all subsequent model calculations. Fig. 8(b) shows the results for a binary elution on another small 1.5 cm×27.3 cm (bed dimensions) column. Fig. 8(b) shows that the model predictions and the experimental results match very well in terms of retention time, peak width and peak height.

Three larger columns (4.4 cm×29.5 cm, 5.0 cm× 29.5 cm, 5.0 cm ×42 cm in bed dimensions) packed with the same P60 gel were used to compare scale-up predictions using single-component and binary elutions. The scale-up predictions could be calculated using the PC software without the three larger columns being physically in existence, that is to say that the predictions could be done a priori. The results are shown in Figs. 9–11. The parameters used for these figures are listed in Table 4. From these figures it can be concluded that the agreement between the model predictions and the experimental results is very good. The volumetric scale-up factor is about 15.6:1 between the small 1.5 cm×30 cm column and the larger 5.0 cm× 42 cm column.

This scale-up method hinges heavily on the assumption that the small column and the larger column have the same ε_b, ε_p, and ε_p^a and τ_{tor} values. This requires that the two columns have the same packing density which means the two beds should be operated at similar pressures without one column been much more compressed than the other. To

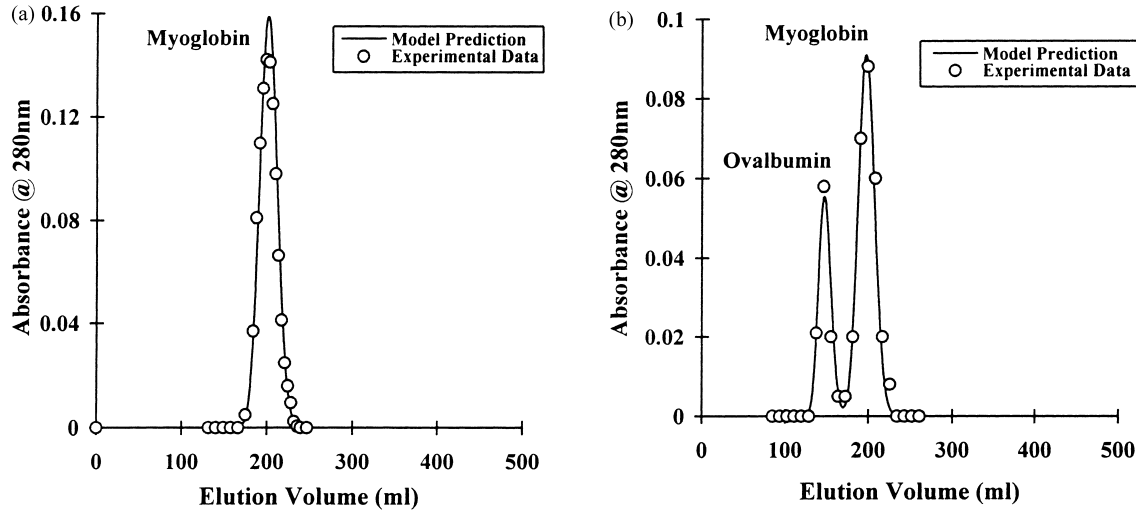

Fig. 9. Comparison between experimental results and model predictions for a large column (4.4 cm×29.5 cm bed dimensions). (a) single component elution; (b) binary elution.

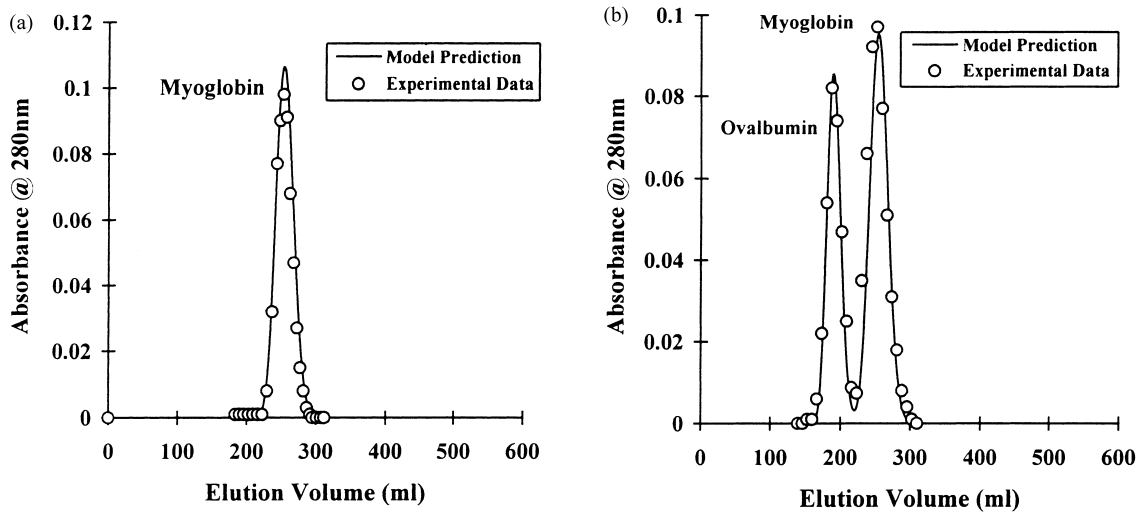

Fig. 10. Comparison between experimental results and model predictions for a large column (5.0 cm×29.5 cm bed dimensions). (a) single component elution; (b) binary elution.

Table 4
Parameter values used in Figs. 8–11

Figures		Proteins	Operation parameters				Simulation parameters					Numerical parameter	
			d (m)	L (m)	$v\times10^4$ (m s^{-1})	$c_0\times10^5$ (mol l^{-1})	Pe_L	Bi	η	τ_{imp}	$k\times10^5$ (m s^{-1})	Nc	Ne
Fig. 8	(a)	Myoglobin	0.015	0.273	1.01	8.9	1498	103	4.1	0.019	1.040	2	24
	(b)	Myoglobin	0.015	0.273	0.48	8.9	1498	80.1	8.5	0.038	0.811	2	30
		Ovalbumin				3.4	1498	341	1.6		0.658		
Fig. 9	(a)	Myoglobin	0.044	0.295	0.73	1.6	1619	92.1	6.1	0.083	0.933	2	24
	(b)	Myoglobin	0.044	0.295	0.71	4.2	1619	91.2	6.2	0.017	0.925	2	30
		Ovalbumin				1.9	1619	388	1.2		0.749		
Fig. 10	(a)	Myoglobin	0.050	0.295	0.71	6.5	1619	91.2	6.3	0.013	0.925	2	24
	(b)	Myoglobin	0.050	0.295	0.76	5.9	1619	93.3	5.8	0.013	0.946	2	30
		Ovalbumin				3.9	1619	397	1.1		0.766		
Fig. 11		Myoglobin	0.050	0.420	0.54	5.9	2305	83.3	11.7	0.045	0.844	2	30
		Ovalbumin				2.3	2305	354	2.3		0.684		

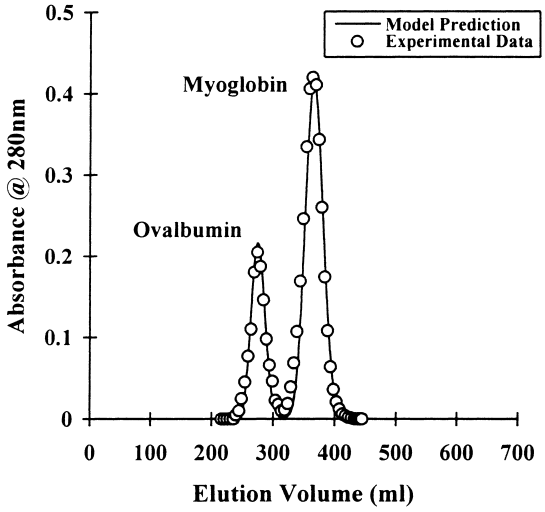

Fig. 11. Comparison between experimental result and model prediction for a large column (5.0 cm×42.0 cm bed dimensions).

maintain the validity of this assumption, the small bench column should be chosen in such a way that it has a similar bed height and operating pressure as the large column. If the bed compression is not a problem, such precautions are relaxed.

Of course for very large columns, it is hard to maintain perfect flow patterns. To compensate for this, a relatively larger bench column should be used such that similar irregular flow patterns occur. Or, a larger τ_{tor} value (than that obtained from a small column with rather good flow patterns) is used for the scale-up predictions of a very large column since a larger τ_{tor} value will result in more diffused peaks. This will compensate poorer performance of a large column due to irregular flows. By doing so, the rate model becomes a semi-empirical model.

6. Conclusions

A procedure was developed using a FORTRAN 77 software program based on a general rate model for the scale-up of SEC columns. Using the elution data from a few simple runs on a small column some physical parameters were obtained. Together with other mass transfer parameters evaluated using existing mass transfer correlations, the elution performance of a much larger column can be predicated a priori. Parameter sensitivities were studied using computer simulation. The validity of the scale-up procedure was demonstrated by scaling up an SEC column from 15 cm×27.3 cm to 5.0 cm×42 cm (bed dimensions) with a volumetric scale-up factor of 15.5 to 1. The FORTRAN 77 software is available free of charge for academic researchers. Both MS-DOS and Windows 95 executable versions are available from the corresponding author. The minimum hardware requirement is a 486 PC with 8 MB of RAM, although a high-end Pentium PC with 16 MB or more RAM is recommended in order to achieve a simulation time in the range of seconds to minutes depending on the stiffness of elution peaks.

7. Nomenclature

Bi	Biot number of mass-transfer of a solute, $kR_p/(\varepsilon_p^a D_p)$
C	adjustable correlation parameter
C_0	concentration of a solute used for nondimensionalization, $\max\{C_f(t)\}$ (mol l^{-1})
C_b	concentration of a solute in the bulk-fluid phase(mol l^{-1})
c_b	C_b/C_0
C_f	feed concentration profile of solute (mol l^{-1})
C_p	concentration of a solute in the stagnant-fluid phase inside particle macropores (mol l^{-1})
c_p	C_p/C_0
D_b	axial dispersion coefficient (m^2 s^{-1})
D_m	intraparticle molecular diffusivity (m^2 s^{-1})
D_p	effective diffusivity in particle macropores (m^2 s^{-1})
d	inner diameter of an SEC column (m)
d_m	diameter of a molecule
d_{pore}	macropore diameter of a particle
F^{ex}	size exclusion factor of a solute (F^{ex}=0 means complete exclusion)
k	film mass transfer coefficient of a solute (m s^{-1})
K_{sec}	distribution coefficient of a solute
L	column length (m)
MW	molecular weight of a solute
N	Avogadro's number, 6.023×10^{23} molecules per mole
Nc	number of interior collocation points
Ne	number of quadratic elements
Pe_L	Peclet number of axial dispersion for a solute, vL/D_b
Q	mobile phase volumetric flow rate (m^3 s^{-1})
R	radial coordinate for a particle in spherical coordinate system
r	R/R_p
R_m	radius of a molecule (m)
R_p	particle radius (m)
Re	Reynolds number in the bulk-fluid phase, $(2R_p)v\varepsilon_b\rho/\mu$
Sc	Schmidt number, $\mu/(D_m\rho)$
Sh	Sherwood number, $k(2R_p)/D_m$
T	absolute temperature (K)
t	dimensional time (t=0 is the moment a sample enters a column) (s)
t_0	retention time of a very small molecule that can penetrate all macropores (s)
t_d	retention time of totally excluded large molecules, such as blue dextran (s)
t_R	retention time of a solute (s)

v interstitial velocity, $4Q/(\pi d^2\varepsilon_b)$ (m s^{-1})
V_0 column void volume (m^3)
V_e solute elution volume (m^3)
$V_{e,0}$ Elution volume at retention time t_0 (m^3)
$V_{e,d}$ Elution volume at retention time t_d (m^3)
$V_{e,R}$ Elution volume at retention time t_R (m^3)
V_{samp} Sample volume (l)
v_s partial specific volume of a molecule (m^3 kg^{-1})
V_t total volume of liquid phase in the column (m^3)
Z column axial coordinate in cylindrical coordinate system
z Z/L

Greek letters

η dimensionless group, $\varepsilon_p^a D_p L/(R_p^2 v)$
κ Boltzmann's constant, 1.38×10^{-23} (J K^{-1})
λ ratio of the solute molecular diameter to the pore diameter, d_m/d_{pore}
λ_0 ratio of the solute molecular diameter to the pore diameter when the solute is completely excluded
μ mobile phase viscosity (Pa s)
ξ dimensionless constant, $3Bi\eta(1-\varepsilon_b)/\varepsilon_b$
ρ density of solvent (kg m^{-3})
τ dimensionless time, vt/L
τ_{imp} dimensionless time duration for a rectangular pulse of the sample, $4V_{samp}/(\pi d^2 L\varepsilon_b)$
τ_{tor} pore tortuosity
ε_b bed void volume fraction
ε_p particle porosity
ε_p^a accessible particle porosity

References

[1] L. Hagel, Peak capacity of columns for size-exclusion chromatography, J. Chromatogr. 591 (1992) 47–54.
[2] G.L. Hagnauer, Preparative size exclusion chromatography, in: B.A. Bidilingmeyer (Ed.), Preparative Liquid Chromatography, J. Chromatogr. Library, vol. 38, 1987, pp. 289–333.
[3] J.C. Moore, Gel permeation chromatography I, new method for molecular weight distribution of high polymers, J. Polym. Sci. Pt. B 2 (1964) 835–843.
[4] T. Burnouf, Integration of chromatography with traditional plasma protein fractionation methods, Bioseparation 1 (1991) 383–396.
[5] S. Yamamoto, Estimation of optimum fractionation conditions in liquid chromatograpy (in Japanese), Kemikaru Enjiniyaringu. 36 (1991) 513–517.
[6] S.M. Wheelwright, Protein Purification: Design and Scale up of Downstream Processing, Hanser Publishers, Munich, 1991, pp. 204–215.
[7] H.G. Barth, B.E. Boyes, C. Jackson, Size exclusion chromatography, Anal. Chem. 66 (1994) 595R–620R.
[8] H.G. Barth, B.E. Boyes, C. Jackson, Size exclusion chromatography, Anal. Chem. 68 (1996) 445R–466R.
[9] H.G. Barth, B.E. Boyes, Size exclusion chromatography, Anal. Chem. 64 (1992) 428R–442R.
[10] R.M. Chicz, F. Regnier, Guide to protein purification, in: M.N. Deuthtscher (Ed.), Methods in Enzymology, vol. 182, 1990, pp. 392–421.
[11] W.W. Yau, J.J. Kirkland, D.D. Bly, Size-exclusion liquid chromatography, in: P.R. Brown, R.A. Hartwick (Eds.), High Performance Liquid Chromatography, Wiley, New York, 1989.
[12] T. Gu, Mathematical Modeling and Scale-up of Liquid Chromatography, Springer, Berlin, New York, 1995, pp. 9–38.
[13] D.H. Kim, A.F. Johnson, Computer model for gel permeation chromatography of polymers, in: T. Provder (Ed.), Size-Exclusion Chromatography: Methodology and Characterization of Polymers and Related Materials, ACS Symp. Series, 245, 1984, pp. 25–45.
[14] Y.M. Koo, P.C. Wankat, Sep. Sci. Technol. 23 (1988) 413–427.
[15] W.W. Yau, J.J. Kirkland, D.D. Bly, Modern size-exclusion liquid chromatography, in: P.R. Brown, R.A. Hartwick (Eds.), High Performance Liquid Chromatography, Wiley, New York, 1979, p. 89.
[16] A.I. Liapis, Modeling affinity chromatography, Sep. Purif. Meth. 19 (1990) 133–210.
[17] B.H. Arve, A.I. Liapis, Modeling and analysis of elution stage biospecific adsorption in fixed beds, Biotech. Bioeng. 320 (1987) 638–649.
[18] Q. Yu, N.-H.L. Wang, Computer simulation of the dynamics of multicomponent ion exchange and adsorption in fixed-beds-gradient-directed moving finite element method, Comp. Chem. Eng. 13 (1989) 915–926.
[19] P.N. Brown, G.D. Byrne, A.C. Hindmarsh, VODE: A variable coefficient ODE solver, SIAM J. Sci. Stat. Comput. 10 (1989) 1038–1051.
[20] S.F. Chung, C.Y. Wen, Longitudinal dispersion of liquid flowing through fixed and fluidized beds, AIChE J. 14 (1968) 857–866.
[21] C.N. Satterfield, C.K. Colton, W.H. Pither, Restricted diffusion in liquids within fine pores, AIChE J. 19 (1973) 628–635.
[22] P.M. Boyer, T. Hsu, Experimental studies of restricted protein diffusion in an agarose matrix, AIChE J. 38 (1992) 259–272.
[23] C.N. Satterfield, T.K. Sherwood, The Role of Diffusion in Catalysis, Addison-Wesley, London, 1963, p. 20.
[24] R.B. Bird, W.E. Steward, E.N. Lightfoot, Transport Phenomena, Wiley, New York, 1960, p. 514.
[25] A.G. Marshall, Biophysical Chemistry: Principles, Techniques, and Applications, Wiley, New York, 1978, p. 201.
[26] C. Tanford, Physical Chemistry of Macromolecules, Wiley, New York, 1961, pp. 336–359.
[27] A. Polson, Some aspects of diffusion in solution and a definition of a colloidal particle, J. Phys. Colloid Chem. 54 (1950) 649–652.
[28] G. Stegeman, J.C. Kraak, H.J. Poppe, Hydrodynamic and size-exclusion chromatography of polymers on porous particles, J. Chromatogr. 550 (1991) 721–739.
[29] E.J. Wilson, C.J. Geankoplis, Liquid mass-transfer at very low Reynolds number in packed beds, I. & E.C. Fundamentals 5 (1966) 9–14.
[30] S. Hussain, M.S. Mehta, J.I. Kaplan, P.L. Dubin, Experimental evaluation of conflicting models for size exclusion chromatography, Anal. Chem. 63 (1991) 1132–1138.